Proceedings of the 11th European Wave and Tidal Energy Conference 6-11th Sept 2015, Nantes, France

On the solution of multi-body wave energy converter motions using pseudo-spectral methods

Francesco Paparella[#1], Giorgio Bacelli[§2], Mícheál Ó'Catháin[&3], John V. Ringwood[#4]
[#]Center for Ocean Energy Research (COER)
Maynooth University, Co. Kildare, Ireland
E-mail: [1]fpaparella@eeng.nuim.ie, [4]john.ringwood@eeng.nuim.ie
[§]Sandia National Laboratories, Albuquerque NM, USA*
E-mail: [2]gbacelli@sandia.gov
[&]SSE Generation Development, Dublin, Ireland
E-mail: [3]micheal.ocathain@sserenewables.com

***Abstract*—Multi-body wave energy converters are composed of several bodies interconnected by joints. Two different formulations are adopted to describe the dynamics of multi-body systems: the Differential and Algebraic Equations (DAEs) formulation and the Ordinary Differential Equations (ODEs) formulation. While the number of variables required for the description of the dynamics of a multi-body system is greater in the DAE formulation than in the ODE formulation, the ODE formulation involves an extra computational effort in order to describe the dynamics of the system with a smaller number of variables. In this paper, pseudo-spectral methods are applied in order to solve the dynamics of multi-body wave energy converters using both DAE and ODE formulations. Apart from providing a solution to the dynamics of multi-body systems, pseudo-spectral methods provide an accurate and efficient formulation for the control of multi-body wave energy converters. As an application example, this paper focuses on the dynamic modeling of a two-body hinge-barge device. Wave-tank tests were carried out on the device in order to validate the DAE and ODE formulation against experimental data. The comparison between pseudo-spectral methods and a method based on the integration of the equations of motion, e.g. the Runge-Kutta method, showed that pseudo-spectral methods are computationally more stable and they require a less computational effort for short time steps.**

***Index Terms*—Multi-body wave energy converters, pseudo-spectral methods, model-based control**

I. Introduction

Multi-body wave energy converters are made of an assemble of bodies connected together by different type of joints. The motion of each body is restrained by the kinematic constraints introduced by the joints. Two different formulations can be used to describe the dynamics of a multi-body system: the Differential and Algebraic Equations (DAEs) and the Ordinary Differential Equations (ODEs) formulation. In the DAE formulation, a set of redundant n *generalized* coordinates is used to describe the dynamics of the system, and the equations of motion result in $2n$ differential and m constraint equations. Also, m unknowns called Lagrange multipliers are added into the differential equations. The Lagrange multipliers are algebraic variables, so that their time derivative is not present in the equations. The resulting system is a set of DAEs for the generalized coordinates and Lagrange multipliers.

In the ODE formulation, the generalized coordinates are expressed with respect to a set of $(n-m)$ *independent* coordinates, also called degrees of the freedom, by means of the constraint equations. Therefore, the DAE system can be transformed into a reduced number of $2(n-m)$ ordinary differential equations (ODEs) for the independent coordinates with elimination of the Lagrange multipliers.

Regarding the solution techniques for DAE systems, index reduction techniques combined with backwardward difference methods (BDFs) have been proposed in [1]. The index of DAE systems made of the Euler-Lagrange equations is reduced from three to two, and then a variable-order, variable-step BDF method is applied to the resulting system of equations.

Alternatively, the DAE system can be reduced to an ODE system by means of an appropriate transformation of coordinates. In Maggi's formulation [2], the generalized velocities are expressed in terms of the kinematic characteristics, which are the velocities of the degrees of freedom. Then, the Euler-Lagrange equations are derived for the kinematic characteristics with elimination of the Lagrange multipliers by means of the null-space of the constraint matrix [3], [4]. In the Index-1 formulation [5], the Euler-Lagrange equations for the generalized coordinates, together with the constraints at the acceleration level, form an Index-1 system of DAEs which can be solved for the generalized coordinates and Lagrange multipliers. Then, the accelerations are integrated in order to obtain the positions and velocities of the generalized coordinates. In the Udwadia and Kalabas Formulation (UKF) [6], a more compact form of the Index-1 formulation was derived by means of the Moore-Penrose Generalized Inverse (MPGI). In the Null Space Formulation (NSF) [5], [7], [8], the Lagrange multipliers that appear in the Index 1 formulation are eliminated from the Euler-Lagrange equations by means of the null space introduced in Maggi's formulation. Therefore, a system of second order ODEs for the generalized coordinates is obtained.

The number of variables needed to describe the dynamics of a constrained system in the DAE formulation is $2n+m$ (n gen-

*Giorgio Bacelli has contributed to the work presented in this paper when he was at Maynooth University

eralized position, n generalized velocities and m Lagrange's multipliers), while, for the ODE formulation, the number of variables is reduced to $2n$ for the Index-1 formulation, NSF and UKF, and $2(n-m)$ for Maggi's formulation. However, the reduction of the number of variables requires an extra computational effort; in Maggi's and the NSF formulation the computation of the null space of the constraint matrix is required, while, in the UKF formulation, MPGIs are calculated. Nevertheless, the matrices in the DAE formulation are characterized by a high sparsity, so that efficient solution techniques can be used [9], [10].

Furthermore, the formulations that enforce the constraints at the velocity level, as in Maggi's formulation, or at the acceleration level, e.g. Index 1 or Null Space formulation, can present a drift of the constraint equations due to numerical approximations [11]. Constraint violation stabilization techniques are used together with other solution techniques in the attempt to remove the drift of the constraint equations. In [12], Baugmarte's method is proposed, which is a stabilization technique based on control theory. In [13], Baugmarte's method is used together with an Index-1 formulation, resulting in a more efficient formulation than the coordinate partitioning approach. The staggered stabilization [14] and augmented Lagrangian formulation [15] are examples of stabilization techniques that are based on penalty terms for the constraint equations added into the Lagrangian of the system.

The constraint violation elimination techniques are more effective in the satisfaction of the constraint equations than the constraint violation stabilization techniques. In [16], a method to obtain an accurate satisfaction of the constraint equations is developed. The method computes the generalized positions and velocities at each time step from the integration of the equations of motion, without considering the constraint equations. Then, a gradient based technique is used to update the generalized positions and velocities so that the constraint equations are satisfied.

In this paper, pseudo-spectral (PS) methods are applied to both the DAE and ODE formulations in order to obtain the solution for the dynamics of a multi-body system. PS methods are a subset of the class of techniques used for the discretisation of integral and partial differential equations known as mean weighted residuals [17], [18]. Apart from providing a solution for the dynamics of a multi-body system, PS methods can also be used to efficiently solve an optimal control problem for the device [19].

The remainder of the paper is organized as follows: in Section 2, the DAE and ODE formulation are applied to a multi-body system, while, in Section 3, PS methods are used to obtain the solution of the dynamics of a multi-body system. In Section 4, a two-body hinge-barge device is considered as a case study, and the DAE and ODE formulations are applied in order to derive the equations of motion. Finally, in Section 5, the DAE and ODE formulations applied to the device are compared against tank test data to verify their validity.

II. Equations of Motion of a Multi-Body System

A. Reference frames

For the description of the motion of a body in space, six coordinates are required: three coordinates for position and three coordinates for rotation. For the analysis of multi-body systems, two types of coordinate frames are defined: the *global* or *inertial* frame and the *body* frame. The global frame is fixed to a point in space, and therefore its position and orientation are constant in time. The body frame is attached to a point of the body, and its position and orientation change with time. A body frame is assigned to each body composing a multi-body system. In Figure 1, a free floating unconstrained body k is represented together with a global frame $X_iY_iZ_i$ and a body frame $X_bY_bZ_b$. The vector $\mathbf{p}_{i,b_k} \in \mathbb{R}^{3\times 1}$ represents the position of the origin of the body frame O_{b_k} with respect to the point i. The components of the vector $\mathbf{p}_{i,b_k}$ can be expressed from the body frame to the global frame by using the following transformation:

$$\mathbf{p}^i_{i,b_k} = \mathbf{R}^i_b(\mathbf{\Theta}_k)\mathbf{p}^b_{i,b_k} \tag{1}$$

where the vectors $\mathbf{p}^b_{i,b_k}$ and $\mathbf{p}^i_{i,b_k}$ represent the position vector of O_{b_k} with respect to the point i expressed in the body frame and global frame, respectively. The matrix $\mathbf{R}^i_b(\mathbf{\Theta}_k) \in \mathbb{R}^{3\times 3}$ used for the transformation of coordinates is a function of the vector of Euler angles $\mathbf{\Theta}_k = [\phi\ \theta\ \psi]^T$, where ϕ is the roll angle, θ is the pitch angle and ψ is the yaw angle of the body [20]. The velocities of the Euler angles can be obtained from the angular velocity vector $\boldsymbol{\omega}^b_{i,b}$ expressed in the body frame coordinates as follows:

$$\dot{\mathbf{\Theta}}_k = \mathbf{T}(\mathbf{\Theta}_k)\boldsymbol{\omega}^b_{i,b_k} \tag{2}$$

where the matrix $\mathbf{T}(\mathbf{\Theta}_k)$ is a function of Euler angles, and it can be obtained by linear superposition of the rotations of the body frame around its axis [20].

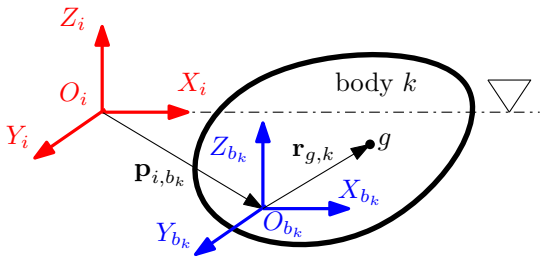

Fig. 1. A free floating unconstrained body k, where $X_iY_iZ_i$ and $X_bY_bZ_b$ represent the global and body reference frames, respectively.

B. Dynamics of an unconstrained body

The Newton-Euler equations of motion for a free floating unconstrained body are represented as a system of first-order integro-differential equations which are given as follows [20]:

$$\dot{\mathbf{q}}_k = \mathbf{J}^{b_k}(\boldsymbol{\Theta})\mathbf{v}_k \tag{3}$$

$$\mathbf{M}^{b_k}\dot{\mathbf{v}}_k + \mathbf{B}^{b_k}\mathbf{v}_k = -\mathbf{G}^{b_k}\boldsymbol{q}_k - \mathbf{M}_{\infty}^{b_k}\dot{\mathbf{v}}_k - \int_{-\infty}^{t}\mathbf{K}_{rad}^{b_k}(t-\tau)\mathbf{v}_k, d\tau + \mathbf{f}_{wave}^{b_k} + \mathbf{f}_{ext}^{b_k} \tag{4}$$

where:

$$\mathbf{q}_k = [\mathbf{p}^{i^T}_{i,b_k}\ \boldsymbol{\Theta}_k^T]^T \tag{5}$$

$$\mathbf{v}_k = [\mathbf{v}^{b^T}_{i,b_k}\ \boldsymbol{\omega}^{b^T}_{i,b_k}]^T \tag{6}$$

$$\mathbf{J}^{b_k}(\boldsymbol{\Theta}) = \begin{bmatrix}\mathbf{R}_b^i(\boldsymbol{\Theta}_k) & \mathbf{0}_{3\times3}\\ \mathbf{0}_{3\times3} & \mathbf{T}(\boldsymbol{\Theta}_k)\end{bmatrix} \tag{7}$$

$$\mathbf{M}^{b_k} = \begin{bmatrix}m_k\mathbf{I}_{3\times3} & -m_k\mathbf{S}(\mathbf{r}_{g,k})\\ m_k\mathbf{S}(\mathbf{r}_{g,k}) & \mathbf{I}_{b_k}\end{bmatrix} \tag{8}$$

$$\mathbf{B}^{b_k} = \begin{bmatrix}m_k\mathbf{S}(\boldsymbol{\omega}^b_{i,b_k}) & -m_k\mathbf{S}(\boldsymbol{\omega}^b_{i,b_k})\mathbf{S}(\mathbf{r}_{g,k})\\ m_k\mathbf{S}(\mathbf{r}_{g,k})\mathbf{S}(\boldsymbol{\omega}^b_{i,b_k}) & -\mathbf{S}(\mathbf{I}_{b_k}\boldsymbol{\omega}^b_{i,b_k})\end{bmatrix} \tag{9}$$

$$\mathbf{f}_{wave}^{b_k} = \int_{-\infty}^{\infty}\mathbf{K}_{wave}^{b_k}(t-\tau)\eta(\tau), d\tau \tag{10}$$

$$\mathbf{f}_{ext}^{b_k} = \mathbf{f}_{PTO}^{b_k} + \mathbf{f}^{b_k} \tag{11}$$

where m_k is the mass of the body, $\mathbf{r}_{g,k}$ is the distance vector of center of mass from origin of body frame, $\mathbf{I}_{b_k}$ is the inertia matrix of the body around the origin of the body frame, $\mathbf{M}^{b_k}$ is the rigid-body inertia matrix of the body, $\mathbf{B}^{b_k}$ is the Coriolis-Centripetal matrix, $\mathbf{B}_{visc}^{b_k}$ is the linearized viscous damping, $\mathbf{G}^{b_k}$ is the hydrostatic matrix, $\mathbf{f}_{wave}^{b_k}$ is the vector of the excitation forces due the action of the waves on the body, $\mathbf{f}_{PTO}^{b_k}$ is the force vector due to Power Take-Off (PTO) system, $\mathbf{f}^{b_k}$ is the vector of forces vector due to moorings, hinge-friction, etc. , $\mathbf{K}_{rad}^{b_k}$ is the impulse response function of radiation forces, $\mathbf{K}_{wave}^{b_k}$ is the impulse response function of wave excitation forces, $\mathbf{M}_{\infty}^{b_k}$ is the added mass at infinity, η is the wave elevation and $\mathbf{S}$ is skew-symmetric matrix for the cross-product $\mathbf{a}\times\mathbf{b} := \mathbf{S}(\mathbf{a})\mathbf{b}$.

The terms on the left-hand side of equation (4) represent the rigid-body dynamics of the unconstrained body expressed about the origin of the body frame $X_bY_bZ_b$. The hydrodynamic parameters $\mathbf{G}^{b_k}$, $\mathbf{M}_{\infty}^{b_k}$, $\mathbf{K}_{rad}^{b_k}$ and $\mathbf{K}_{wave}^{b_k}$ are computed by means of the boundary element software WAMIT [21], which computes all the quantities in the hydrodynamic h-frame. The transformation matrix $\mathbf{R}_b^h$ is used to convert the hydrodynamic parameters from the h-frame to the body frame [22]. Under the assumption of small oscillations of the body frame with respect to the h-frame, the matrix $\mathbf{R}_b^h$ reduces to the identity matrix $\mathbf{I}_{3\times3}$.

C. DAE formulation for N interconnected bodies

In case of N interconnected bodies, m algebraic equations are required in order to describe the constraints introduced by the joints. The constraint equations can be represented as follows:

$$\mathbf{C}(\mathbf{z}, t) = 0 \tag{12}$$

where $\mathbf{z} = [\mathbf{z}_1^T\ ..\ \mathbf{z}_N^T]^T \in \mathbb{R}^{(6\times N)\times1}$ and $\mathbf{z}_k = [\mathbf{p}^{b^T}_{i,b_k}\ \boldsymbol{\Theta}_k^T]^T$, with $k = 1, ..N$. The constraint equations (12) are considered to be *holonomic*, since the generalized velocities do not appear in the equations. An additional term, representing the constraint forces, is added into the Newton-Euler equations of motion. The constraint forces are represented by a set of m variables called *Lagrange* multipliers $\boldsymbol{\lambda}$, which are algebraic variables, since their time derivatives do not appear in the equations of motion. Thus, the equations of motion of a system composed by N interconnected bodies can be represented by a set of DAEs, given as follows [23]:

$$\dot{\mathbf{q}} = \mathbf{J}(\boldsymbol{\Theta})\mathbf{v} \tag{13}$$

$$\mathbf{M}\dot{\mathbf{v}} + \mathbf{B}\mathbf{v} + \mathbf{C}_z^T\boldsymbol{\lambda} = -\mathbf{G}\mathbf{q} - \mathbf{M}_{\infty}\dot{\mathbf{v}} - \int_{-\infty}^{t}\mathbf{K}_{rad}(t-\tau)\mathbf{v}, d\tau + \mathbf{f}_{wave} + \mathbf{f}_{ext} \tag{14}$$

$$\mathbf{C}(\mathbf{z}, t) = 0 \tag{15}$$

where:

$$\mathbf{q} = [\mathbf{q}_1^T\ \mathbf{q}_2^T\ ..\ \mathbf{q}_N^T]^T \tag{16}$$

$$\mathbf{v} = [\mathbf{v}_1^T\ \mathbf{v}_2^T\ ..\ \mathbf{v}_N^T]^T \tag{17}$$

$$\mathbf{J}(\boldsymbol{\Theta}) = \text{diag}(\mathbf{J}^{b_1}(\boldsymbol{\Theta}), .., \mathbf{J}^{b_N}(\boldsymbol{\Theta}) \tag{18}$$

$$\mathbf{M} = \text{diag}(\mathbf{M}^{b_1}, .., \mathbf{M}^{b_N}) \tag{19}$$

$$\mathbf{B} = \text{diag}(\mathbf{B}^{b_1}, .., \mathbf{B}^{b_1}) \tag{20}$$

$$\mathbf{G} = \text{diag}(\mathbf{G}^{b_1}, .., \mathbf{G}^{b_1}) \tag{21}$$

$$\mathbf{M}_{\infty} = \text{diag}(\mathbf{M}_{\infty}^{b_1}, .., \mathbf{M}_{\infty}^{b_N}) \tag{22}$$

$$\mathbf{f}_{wave} = [\mathbf{f}_{wave}^{b_1{}^T}.. \mathbf{f}_{wave}^{b_N{}^T}]^T \tag{23}$$

$$\mathbf{f}_{ext} = [\mathbf{f}_{ext}^{b_1{}^T}.. \mathbf{f}_{ext}^{b_N{}^T}]^T \tag{24}$$

The matrix $\mathbf{C}_z$ represents the partial derivative of the constraint equations with respect to the vector of generalized positions $\mathbf{z}$. In the DAE formulation, the total number of variables required for describing the motion of N interconnected bodies is $2\times(6\times N)+m$, i.e. $6\times N$ positions, $6\times N$ velocities and m Lagranges multipliers.

D. ODE formulation for N interconnected bodies

As an alternative to the DAE formulation, the dynamics of N interconnected bodies can be described by means of a set of $n = (6\times N - m)$ independent coordinates, called *degrees of freedom* (DoF). The vector of generalized velocities $\mathbf{v}$ can be partitioned into dependent velocities $\mathbf{v}_d$, and independent velocities $\mathbf{v}_s$, as follows:

$$\mathbf{v} = \begin{bmatrix}\mathbf{v}_d\\ \mathbf{v}_s\end{bmatrix} \tag{25}$$

The dependent velocities can be expressed with respect to the independent velocities as follows [23]:

$$\mathbf{v}_d = \mathbf{C}_s \mathbf{v}_s = -\mathbf{C}_{\mathbf{q}_d}^{-1} \mathbf{C}_{\mathbf{q}_s} \mathbf{v}_s \tag{26}$$

where $\mathbf{C}_{\mathbf{q}_d}$ and $\mathbf{C}_{\mathbf{q}_s}$ represent the partial derivatives of the constraint equations associated with the dependent and independent coordinates, respectively. Therefore, the vector of generalized velocities $\mathbf{v}$ can be written in terms of the independent velocities $\mathbf{v}_s$, as follows:

$$\mathbf{v} = \mathbf{P}\mathbf{v}_s = \begin{bmatrix} \mathbf{C}_s \\ \mathbf{I} \end{bmatrix} \mathbf{v}_s \tag{27}$$

where $\mathbf{I}$ is the identity matrix of dimension n. The time derivative of the generalized velocities can be expressed as follows:

$$\dot{\mathbf{v}} = \mathbf{P}\dot{\mathbf{v}}_s + \dot{\mathbf{P}}\mathbf{v}_s \tag{28}$$

By substituting equation (27) and (28) into equation (14), and multiplying the left-hand side and right-hand side of the resulting equation by $\mathbf{P}^T$, the following system of first order integro-differential equations is obtained:

$$\dot{\mathbf{q}}_s = \mathbf{v}_s \tag{29}$$

$$\mathbf{M}_s\dot{\mathbf{v}}_s + \mathbf{B}_s\mathbf{v}_s = -\mathbf{G}_s\mathbf{q}_s - \mathbf{M}_{\infty,s}\dot{\mathbf{v}}_s - \int_{-\infty}^{t} \mathbf{K}_{rad,s}(t-\tau)\mathbf{v}_s, d\tau + \mathbf{f}_{wave,s} + \mathbf{f}_{ext,s} \tag{30}$$

where:

$$\mathbf{M}_s = \mathbf{P}^T\mathbf{M}\mathbf{P} \tag{31}$$
$$\mathbf{B}_s = \mathbf{P}^T\mathbf{B}\mathbf{P} + \mathbf{P}^T\mathbf{M}\dot{\mathbf{P}} + \mathbf{P}^T\mathbf{M}_\infty\dot{\mathbf{P}} \tag{32}$$
$$\mathbf{G}_s = \mathbf{P}^T\mathbf{G}\mathbf{P} \tag{33}$$
$$\mathbf{M}_{\infty,s} = \mathbf{P}^T\mathbf{M}_\infty\mathbf{P} \tag{34}$$
$$\mathbf{K}_{rad,s} = \mathbf{P}^T\mathbf{K}_{rad}\mathbf{P} \tag{35}$$
$$\mathbf{f}_{wave,s} = \mathbf{P}^T\mathbf{f}_{wave} \tag{36}$$
$$\mathbf{f}_{ext,s} = \mathbf{P}^T\mathbf{f}_{ext} \tag{37}$$

Thus, the equations of motion of a system composed by N interconnected bodies can be represented by a set of ODEs for the independent coordinates. In the ODE formulation, the total number of variables required for describing the motion is $2n$ (n positions and n velocities).

III. Pseudo-spectral methods for approximating the motion

In the following section, PS methods are applied to compute an approximate solution of the integro-differential equations obtained for the DAE and ODE formulations. For control purposes, pseudo-spectral methods result in less complex and more accurate solutions than control techniques based on the integration of the equations of motion over the time horizon, e.g. the multiple shooting approach. The positions and velocities that appear in the equations of motion obtained for the DAE and ODE formulations can be approximated with a linear combination of basis functions. Given the periodic nature of the variables associated with the problem, non-zero mean trigonometric polynomials (truncated Fourier series) represent a sensible choice for the approximation of positions and velocities. Therefore, the ith components of the position and velocity vector are given as follows:

$$q_i(t) \approx q_i^{N_x}(t) = \sum_{k=1}^{N_x} x_{i,k}^{q,c} cos(k\omega_0 t) + x_{i,k}^{q,s} sin(k\omega_0 t) = \mathbf{\Phi}(t)\hat{\mathbf{x}}_i^q \tag{38}$$

$$v_i(t) \approx v_i^{N_x}(t) = \sum_{k=1}^{N_x} x_{i,k}^{v,c} cos(k\omega_0 t) + x_{i,k}^{v,s} sin(k\omega_0 t) = \mathbf{\Phi}(t)\hat{\mathbf{x}}_i^v \tag{39}$$

where $i = 1, .., 6N$ and $i = 1, .., n$ for the DAE and ODE formulations, respectively. The parameter N_x is the order of expansion for the position and velocity of the states. The vector of the coefficients $\hat{\mathbf{x}}_i^q$ and $\hat{\mathbf{x}}_i^v$ of the approximated ith components of the position and velocity vector are given as follows:

$$\hat{\mathbf{x}}_i^q = \begin{bmatrix} x_{i,1}^{q,c} & x_{i,1}^{q,s} & x_{i,2}^{q,c} & x_{i,2}^{q,s} & .. & x_{i,N_x}^{q,c} & x_{i,N_x}^{q,s} \end{bmatrix}^T \tag{40}$$

$$\hat{\mathbf{x}}_i^v = \begin{bmatrix} x_{i,1}^{v,c} & x_{i,1}^{v,s} & x_{i,2}^{v,c} & x_{i,2}^{v,s} & .. & x_{i,N_x}^{v,c} & x_{i,N_x}^{v,s} \end{bmatrix}^T \tag{41}$$

and the vector of the basis function $\mathbf{\Phi}(t)$ is given as follows:

$$\mathbf{\Phi}(t) = \begin{bmatrix} cos(\omega_0 t) & sin(\omega_0 t) & .. & cos\left(N_x\omega_0 t\right) & sin\left(N_x\omega_0 t\right) \end{bmatrix}^T \tag{42}$$

where $\omega_0 = 2\pi/T$ is the fundamental frequency. The derivatives of the ith components of the position and velocity vector are, respectively,

$$\dot{q}_i^{N_x}(t) = \dot{\mathbf{\Phi}}(t)^T\hat{\mathbf{x}}_i^q = \mathbf{\Phi}(t)^T\mathbf{D}_\phi\hat{\mathbf{x}}_i^q \tag{43}$$
$$\dot{v}_i^{N_x}(t) = \dot{\mathbf{\Phi}}(t)^T\hat{\mathbf{x}}_i^v = \mathbf{\Phi}(t)^T\mathbf{D}_\phi\hat{\mathbf{x}}_i^v \tag{44}$$

where $\mathbf{D}_\phi \in \mathbb{R}^{2N_x \times 2N_x}$ is a block diagonal matrix, with the k-th block is given as follows:

$$\mathbf{D}_{\phi,k} = \begin{bmatrix} 0 & k\omega_0 \\ -k\omega_0 & 0 \end{bmatrix} \tag{45}$$

Regarding the DAE formulation, substituting the approximated states (38), (39) and their time derivatives (43), (44) into the equations of motion (13)-(15), yields the following equations of motion in residual form:

$$r_i^q(t) = \mathbf{\Phi}(t)\mathbf{D}_\phi \hat{\mathbf{x}}_i^q - \sum_{p=1}^{6N} J_{i,p}\mathbf{\Phi}(t)\hat{\mathbf{x}}_p^v \tag{46}$$

$$\begin{aligned} r_i^v(t) = &\sum_{p=1}^{6N} M_{i,p}\mathbf{\Phi}(t)\mathbf{D}_\phi \hat{\mathbf{x}}_p^v + \sum_{p=1}^{6N} B_{i,p}\mathbf{\Phi}(t)\hat{\mathbf{x}}_p^v + \sum_{p=1}^{6N} G_{i,p}\mathbf{\Phi}(t)\hat{\mathbf{x}}_p^q \\ &+ \sum_{p=1}^{6N}\int_{-\infty}^{t} K_{rad_{i,p}}(t-\tau)\mathbf{\Phi}(\tau)\hat{\mathbf{x}}_p^v d\tau + \sum_{p=1}^{m} C_{q_{i,p}}^T \mathbf{\Phi}(t)\hat{\mathbf{x}}_p^\lambda(t) \\ &- f_{wave,i}(t) - f_i(t) \end{aligned} \tag{47}$$

$$r_j^C(t) = C_j(\mathbf{q}, t) \tag{48}$$

with $i = 1, .., 6N$, $j = 1, .., m$, and $J_{i,p}$, $M_{i,p}$, $B_{i,p}$, $G_{i,p}$, $K_{rad_{i,p}}$ and $C_{q_{i,pp}}^T$ are the elements of the matrix $\mathbf{J}(\mathbf{\Theta})$, $\mathbf{M}$, $\mathbf{B}$, $\mathbf{G}$, $\mathbf{K}_{rad}$ and $\mathbf{C}_q^T$, respectively. Regarding the ODE formulation, substituting the approximated states (38), (39) and their time derivatives (43), (44) into the equations of motion (29)-(30), yields the following equations of motion in residual form:

$$r_i^q(t) = \mathbf{\Phi}(t)\mathbf{D}_\phi \hat{\mathbf{x}}_i^q - \mathbf{\Phi}(t)\hat{\mathbf{x}}_i^v \tag{49}$$

$$\begin{aligned} r_i^v(t) = &\sum_{p=1}^{n} M_{s_{i,p}}\mathbf{\Phi}(t)\mathbf{D}_\phi \hat{\mathbf{x}}_p^v(t) + \sum_{p=1}^{n} B_{s_{i,p}}\mathbf{\Phi}(t)\hat{\mathbf{x}}_p^v \\ &+ \sum_{p=1}^{n} G_{s_{i,p}}\mathbf{\Phi}(t)\hat{\mathbf{x}}_p^q + \sum_{p=1}^{n}\int_{-\infty}^{t} K_{rad,s_{i,p}}(t-\tau)\mathbf{\Phi}(\tau)\hat{\mathbf{x}}_p^v d\tau \\ &- f_{wave,s_i}(t) - f_{s_i}(t) \end{aligned} \tag{50}$$

with $i = 1, .., n$, and $M_{s_{i,p}}$, $B_{s_{i,p}}$, $G_{s_{i,p}}$, and $K_{rad,s_{i,p}}$ are the elements of the matrix $\mathbf{M}_s$, $\mathbf{B}_s$, $\mathbf{G}_s$ and $\mathbf{K}_{rad,s}$, respectively. PS methods are applied to compute the coefficients $\hat{\mathbf{x}}_i^q$ and $\hat{\mathbf{x}}_i^v$ that minimize the residuals (46)-(48) and (49)-(50) for the DAE and ODE formulations, respectively [24]. The PS methods force the residuals of the equations of motion to be zero at a certain number of points in time t_k, called *nodes*. If the number of nodes is equal to N_c, then a nonlinear system of $(2 \times 6N + m) \times N_c$ and $2 \times n \times N_c$ equations is solved for the DAE and ODE formulations, respectively. The number of nodes depends on multiple factors, among which the order of the expansion N_x [25].

IV. Case Study: Two-Body Hinge-Barge Device

In the following section, a two-body hinge barge device is considered as a case study. As shown in Figure 2, the device is made of two bodies interconnected by a hinge. Examples of such systems include the McCabe Wave Pump (MWP) [26] and the SeaPower Platform [27]. Generally, hinge-barge devices are made by the interconnection of multiple barges, where the relative pitch motion between barges is used to drive Power TakeOff (PTO) systems in order to convert the energy from the waves into mechanical energy. The damping plate connected to body 1 aims to reduce the vertical motion of body 1, and increase the pitch motion of body 2. The analysis of the motion of the device is restricted to the two dimensional plane $X - Z$. In Figure 2, the device is represented together with the global frame $X_g Z_g$, while the body frames $X_{b1} Z_{b1}$ and $X_{b2} Z_{b2}$ are assigned to body 1 and body 2, respectively. The total number of degrees of freedom of the system is equal to three: the heave displacement z_1 of body 1, the pitch angle θ_1 of body 1, and the pitch angle θ_2 of body 2.

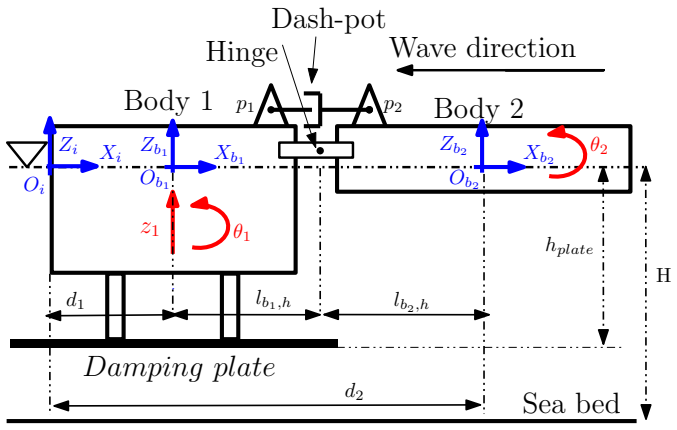

Fig. 2. Two-body hinge barge device, where $X_g Z_g$, $X_{b1} Z_{b1}$ and $X_{b2} Z_{b2}$ represent the global frame, frame of body 1 and body 2, respectively.

A. DAE formulation for a two-body hinge-barge device

In the following subsection, the DAE formulation is applied in order to obtain the equations of motion of a two-body hinge-barge device. The vector of generalized positions considered for the two-body hinge-barge device is given as follows:

$$\mathbf{z} = [\mathbf{z}_1 \ \mathbf{z}_2]^T = [z_{i,b_1}^b \ \theta_1 \ z_{i,b_2}^b \ \theta_2]^T \tag{51}$$

where z_{i,b_k}^b and θ_k are the heaving displacements and pitch angle of body k, respectively, with $k = 1, 2$. In the following, the constraint equations for the two-body hinge-barge device are derived. The hinge between the two barges introduces the following constraint equations:

$$\mathbf{R}_b^i(\theta_1)\left(\begin{bmatrix} d_1 \\ z_{i,b_1}^b \end{bmatrix} + \begin{bmatrix} l_{b1,h} \\ 0 \end{bmatrix}\right) - \mathbf{R}_b^i(\theta_2)\left(\begin{bmatrix} d_2 \\ z_{i,b2}^b \end{bmatrix} + \begin{bmatrix} -l_{b2,h} \\ 0 \end{bmatrix}\right) = 0 \tag{52}$$

where $l_{b_1,h}$ and $l_{b_2,h}$ are the distances of the hinge from O_{b_1} and O_{b_2}, respectively. The rotation matrices $\mathbf{R}_b^i$ are given as follows:

$$\mathbf{R}_b^i(\theta_k) = \begin{bmatrix} c(\theta_k) & -s(\theta_k) \\ s(\theta_k) & c(\theta_k) \end{bmatrix} \tag{53}$$

where $k = 1, 2$. The constraints in equation (52) force the global position of the hinge defined by the coordinates of body 1 to be equal to the global position of the hinge defined by the coordinates of body 2. The matrix of the partial derivatives of constraint equations (52) computed with respect to the

generalized positions and linearized around the equilibrium position, is given as follows:

$$\mathbf{C}_z = \begin{bmatrix} 1 & l_{b_1,h} & -1 & l_{b_2,h} \end{bmatrix} \tag{54}$$

The block matrices $\mathbf{J}_k(\mathbf{\Theta})$ of the transformation matrix $\mathbf{J}(\mathbf{\Theta})$ in equation (18) are given as:

$$\mathbf{J}^{b_k} = \begin{bmatrix} c(\theta_k) & 0 \\ 0 & 1 \end{bmatrix} \tag{55}$$

where $k = 1, 2$. The block matrices $\mathbf{M}_k$ of the rigid-body inertia matrix $\mathbf{M}$ in equation (19) are given as:

$$\mathbf{M}^{b_k} = \begin{bmatrix} m_k & 0 \\ 0 & I_{yy,k} + m_k h_{g,k}^2 \end{bmatrix} \tag{56}$$

where $k = 1, 2$, m_k is the mass of body k, $I_{yy,k}$ is the moment of inertia of body k around the y-axis and $h_{g,k}$ is the distance of the center of mass of body k from point O_{bk} along the z-axis. The block matrices B_k of the coriolis-centripetal matrix $\mathbf{B}$ in equation (20) are given as:

$$\mathbf{B}^{b_k} = \begin{bmatrix} 5 & -m_k \dot{\theta}_k h_{g,k} \\ m_k \dot{\theta}_k h_{g,k} & 5 \end{bmatrix} \tag{57}$$

where $k = 1, 2$. The terms on the main diagonal of the matrix $\mathbf{B}^{b_k}$ are equal to the 5% of the maximum radiation force, and they represent an approximation of the viscous damping acting on the device. The hydrodynamic loads $\mathbf{G}$, $\mathbf{M}_\infty$, $\mathbf{K}_{rad}$ and $\mathbf{f}_{wave}$ in equations (21), (22), (14) and (23) respectively, are obtained by means of the boundary element software WAMIT [21]. The vector of external forces $\mathbf{f}_{ext}$ in equation (24) is given as follows:

$$\mathbf{f}_{ext} = \mathbf{f}_{PTO} + \mathbf{f}_{moor} \tag{58}$$

where $\mathbf{f}_{PTO}$ is the vector of forces due to the PTO system, and $\mathbf{f}_{moor}$ is the vector of loads due to the moorings. As shown in Figure 2, the PTO system can be modeled as a linear dash-pot system connected to points p_1 and p_2. The component of the PTO force along the line connecting points p_1 and p_2 is as follows:

$$F_s = c_{PTO} \dot{l} \tag{59}$$

where c_{PTO} and l are respectively the damping coefficient and length of the dash-pot system. For small displacements of body 1 and 2, the rate of change of the length l can be calculated as follows:

$$\dot{l} = d(\dot{\theta}_1 - \dot{\theta}_2) \tag{60}$$

where d is the vertical distance of points p_1 and p_2 from the center line of the device. The vector of the loads due to the PTO systems acting on the device is given as follows:

$$\mathbf{f}_{PTO} = - \begin{bmatrix} 0 \\ -F_{s1} d \\ 0 \\ F_{s1} d \end{bmatrix} \tag{61}$$

The moorings are assumed to be connected only to body 1, and therefore, the vector $\mathbf{f}_{moor}$ is given as follows [28]:

$$\mathbf{f}_{moor} = -\mathbf{K}_{moor} \mathbf{q} \tag{62}$$

where:

$$\mathbf{K}_{moor} = \begin{bmatrix} k_{moor,1} & 0 & 0 & 0 \\ 0 & k_{moor,2} & 0 & 0 \\ 0 & 0 & 0 & 0 \\ 0 & 0 & 0 & 0 \end{bmatrix} \tag{63}$$

where $k_{moor,k}$, with $k = 1, 2$, are the stiffness coefficients of the moorings.

B. ODE formulation for a two-body hinge-barge device

In the following subsection, the ODE formulation is applied in order to obtain the equations of motion of a two-body hinge-barge device. The vector of independent velocities of the device is given as follows:

$$\mathbf{v}_s = [\dot{z}^b_{i,b_1} \ \dot{\theta}_1 \ \dot{\theta}_2]^T \tag{64}$$

Given the matrix $\mathbf{C}_z$ in equation (54), the transformation matrix $\mathbf{P}$ in equation (27) used to express the relation between the vector of generalized velocities and independent velocities is given as follows:

$$\mathbf{P} = \begin{bmatrix} 1 & 0 & 0 \\ 0 & 1 & 0 \\ 1 & l_{b1,h} & l_{b2,h} \\ 0 & 0 & 1 \end{bmatrix} \tag{65}$$

By means of the matrix $\mathbf{P}$, the quantities defined in equations (31)-(37) can be calculated in order to obtain the equations of motion of the device expressed with respect to the degrees of freedom.

C. A specific two-body hinge-barge device

In this work, a particular two-body hinge-barge device was tested in a wave-tank in order to validate the DAE and ODE formulation against experimental data. In Table I, the parameters of the tested device are reported.

V. Model validation

The two-body hinge-barge device presented in the previous section was tested in a wave tank. Full details on the wave-tank experiments are reported in [29]. A series of regular wave tests was performed for a range of frequencies of the incident wave ω from 2.61 rad/sec to 7.85 rad/secs, with the direction of the waves along the longitudinal direction of the device. The amplitude of the incident wave was set to 60 mm for each test. The advantage of testing the device with

Parameter	Units	Value
Length barge 1	m	1.1
Width barge 1	m	0.67
Height barge 1	m	0.57
Draft barge 1	m	0.37
Length barge 2	m	2.5
Width barge 2	m	0.64
Height barge 2	m	0.12
Draft barge 2	m	0.08
Length damping plate	m	2.2
Width damping plate	m	1.34
h_{plate}	m	1.47
H	m	1.5
$h_{g,2}$	m	0.0175
$h_{g,1}$	m	0.084
$h_{g,2}$	m	0.0175
$l_{b_1,h}$	m	0.78
$l_{b_2,h}$	m	1.48
c_{PTO}	Ns/m	850
$x_{b_1,p1}$	m	0.35
$z_{b_1,p1}$	m	0.1
$x_{b_2,p2}$	m	0.55
$z_{b_2,p2}$	m	0.1
$k_{moor,1}$	N/m	3.5e4
$k_{moor,2}$	N/m	3.5e4
$k_{moor,3}$	N/m	3.5e4

TABLE I
PARAMETERS FOR SPECIFIC TWO-BODY HINGE-BARGE DEVICE

monochromatic waves is that the response of the device can be obtained at each frequency. The heave motion of body 2 was recorded and compared against the response obtained from the DAE and ODE formulations derived in sections IV-A and IV-B, respectively. PS methods were applied to compute an approximated solution for the equations of motion obtained for the DAE and ODE formulations. The order of expansion N_x for the position and velocity of the states is set equal to 1, and the fundamental frequency ω_0 is set equal to the frequency of the incident wave. Simulations of the device were carried out in Matlab running on a PC with a 3.40 GHz quad core processor and 8 GB RAM. In Figure 3, the frequency response of the heave of body 2 obtained from the tank experiments is compared against the response obtained from both the DAE and ODE formulations. As Figure 3 shows, with respect to the tank experiments, the DAE and ODE formulations gives an accurate frequency response of the heave of body 2 for a range of frequencies from 2.61 rad/sec to 5.8 rad/sec. However, for frequencies greater than 5.8 rad/s, both the DAE and ODE formulations give a less accurate response. The total mean squared error across the range of tested frequencies is equal to $1.18 \cdot 10^{-5}\ m^2$ and $1.2 \cdot 10^{-5}\ m^2$ for the DAE and ODE formulation, respectively. By way of example, the time response for the heave of body 2 given by the DAE formulation compared to the tank experiment is shown in Figures 4 and 5, for ω equal to 6.28 rad/s and 2.8 rad/s, respectively.

With regard to the computational time, a comparison between the DAE and ODE formulations, and a method based on the integration of the equations of motion, e.g. the Runge-Kutta method, is made. While the Runge-Kutta method is used to solve both the transient and steady-state response of the device, the DAE and ODE formulations are used to obtain the steady-state response of the device only. It is important to highlight that, at steady-state, the response obtained with the Runge-Kutta method, and DAE and ODE formulations, is the same.

For a simulation time equal to 15 seconds, in Figure 6, the computational time required by the DAE and ODE formulations is compared to the computational time required by the Runge-Kutta method for different sizes of the time step. As Figure 6 shows, the Runge-Kutta method is more efficient than the DAE and ODE formulations for long time steps, while, for the DAE and ODE formulations, the computational time does not change significantly for different sizes of the time step. The DAE and ODE formulations are solved with a fixed number of collocation points, and then, the solution is interpolated along the simulation time for different time steps. Therefore, the computational time required by the DAE and ODE formulation is independent from the simulation time and size of the time step.

While in the Runge-Kutta method the size of the time step is bounded in order to guarantee the stability of the method, PS methods are also stable for longer time steps than 0.1 seconds. For short time steps, the DAE and ODE formulations are computationally faster than the Runge-Kutta method, allowing the simulation of stiff problems, where a small time step is required in order to describe the rapid transients of the solution. Stiffness can be introduced into the dynamic model of a wave energy converter when, for example, the water hammer effects in the PTO system are considered.

It is interesting to note that the ODE formulation is computationally faster than the DAE formulation for all the time steps. The fact that the ODE formulation requires a shorter computational time than the DAE formulation could be significant in the real-time model-based control of the device.

For a time step equal to 0.05 seconds, in Figure 7, the computational time required by the DAE and ODE formulations is compared to the computational time required by the Runge-Kutta method for different simulation times. As Figure 7 shows, the Runge-Kutta method is less efficient than the DAE and ODE formulations for long simulation times.

VI. Conclusions

This paper demonstrates that PS methods are a compact and numerically efficient formulation for solving the dynamics of multi-body wave energy devices. Using a two-body hinge-barge device as a case study, experimental tests with monochromatic waves were carried out in order to validate the use of PS methods for solving the dynamics of the device. Both DAE and ODE PS formulations were applied in order to describe the dynamics of the device, showing good agreement with experimental tests in terms of device motion. However, experimental tests with polychromatic waves are necessary in order to validate PS methods under a wider range of conditions.

While the DAE formulation is superior to the ODE formulation in terms of accuracy of the computed motion of the device, the ODE formulation requires shorter computational times.

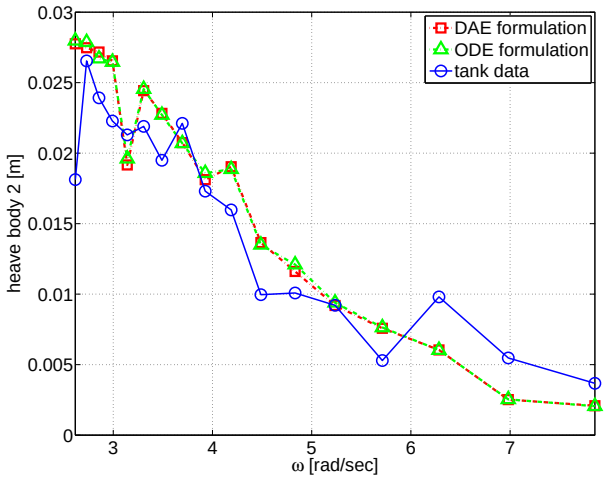

Fig. 3. Frequency response of the heave of body 2 obtained from tank experiments, DAE and ODE formulation for an incident wave of amplitude equal to 60 mm

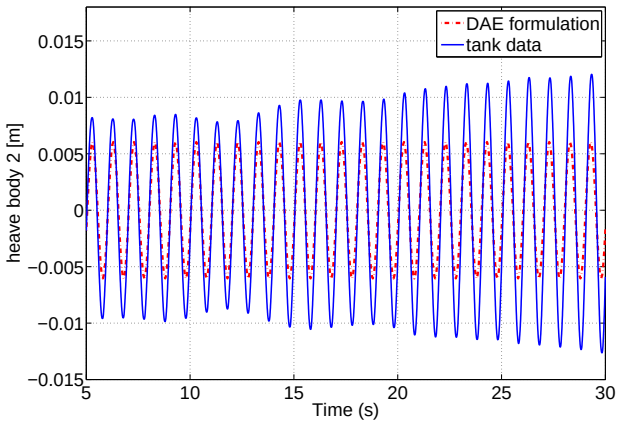

Fig. 4. Time response of the heave of body 2 obtained from tank experiments and DAE formulation for an incident wave of amplitude equal to 60 mm and frequency $\omega = 6.28$ rad/sec

With respect to reference methods based on the integration of the equations of motion, e.g. the Runge-Kutta method, PS methods are computationally more stable and require less computational effort for small time steps. In terms of solution accuracy, PS methods can be less accurate than the Runge-Kutta method, since they compute an approximation of the solution based on a finite number of expansion coefficients.

However, for the optimal control of multi-body wave energy converters, PS methods are generally more efficient than native methods such as Model Predictive Control (MPC), which relies on the simulation capabilities of the integration method in order to compute the optimal solution of the control input. In fact, in order to compute the optimal control input, PS methods only require a small extra computational effort in order to compute the expansion coefficients of the control force, in addition to the expansion coefficients of the state variables.

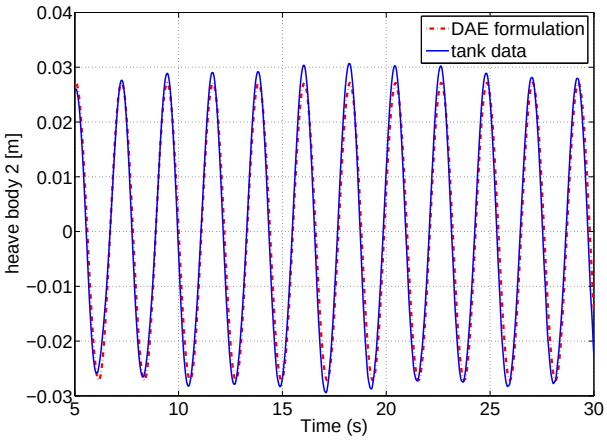

Fig. 5. Time response of the heave of body 2 obtained from tank experiments and DAE formulation for an incident wave of amplitude equal to 60 mm and frequency $\omega = 2.8$ rad/sec

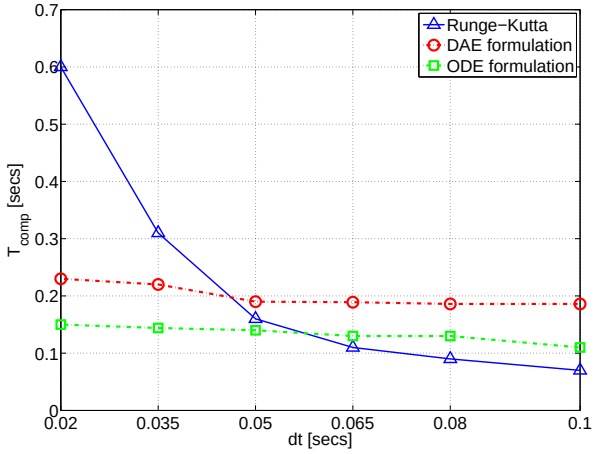

Fig. 6. Computational time required by the Runge-Kutta method, DAE and ODE formulations computed for different time steps and simulation time equal to 15 seconds

ACKNOWLEDGMENT

This paper is based upon work supported by Science Foundation Ireland under Grant No. 12/RC/2302 for the Marine Renewable Ireland (MaREI) centre.

REFERENCES

[1] Gear, C. W., Leimkuhler, B., and Gupta G. K., "Automatic integration of Euler-Lagrange equations with constraints," *J. Comput. Appl. Math.*, vol. 12&13, pp. 77–90, 1985.

[2] Maggi, G. A., *Principii della Teoria Matematica del Movimento Dei Corpi: Corso di Meccanica Razionale*. Ulrico Hoepli, 1896.

[3] Laulusa, A. and Bauchau, O. A., "Review of classical approaches for constraint enforcement in multibody systems," *Journal of Computational and Nonlinear Dynamics*, vol. 3, no. 1, p. 011004 (8 pages), January 2008.

[4] Neimark, J. I. and Fufaev, N. A., *Dynamics of Nonholonomic Systems*. American Mathematical Society, Providence, RI, 1972.

[5] Hemami, H. and Weimer, F. C., "Modeling of nonholonomic dynamic systems with applications," *ASME J. Appl. Mech.*, vol. 48, pp. 177–182, 1981.

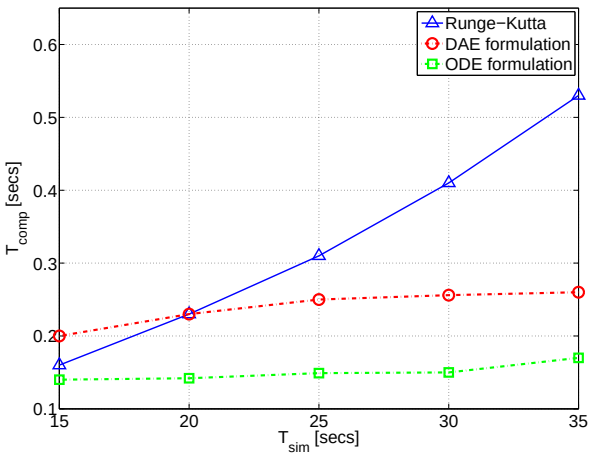

Fig. 7. Computational time required by the Runge-Kutta method, DAE and ODE formulations computed for different simulation times and time step equal to 0.05 seconds

[6] Udwadia, F. E., Kalaba, R. E., and Eun, H. C., "Equations of motion for constrained mechanical systems and the Extended D'Alembert's Principle," *Q. Appl. Math.*, vol. 55, no. 2, pp. 321–331, 1997.

[7] García de Jalón, J., Unda, J., Avello, A., and Jiménez, J. M., "Dynamic analysis of three-dimensional mechanisms in "Natural" coordinates," *ASME J. Mech., Transm., Autom. Des.*, vol. 109, pp. 460–465, 1987.

[8] Unda, J., García de Jalón, J., J., Losantos, F., and Enparantza, R., "A comparative study on some different formulations of the dynamic equations of constrained mechanical systems," *ASME J. Mech., Transm., Autom.Des.*, vol. 109, pp. 466–474, 1987.

[9] Orlandea, N., Chace, M. A., and Calahan, D. A., "A sparsity-oriented approach to the dynamic analysis and design of mechanical systems. Part I," *ASME J. Eng. Ind.*, vol. 99, no. 3, pp. 773–779, 1977.

[10] Orlandea, N., Calahan, D. A., and Chace, M. A., "A sparsity-oriented approach to the dynamic analysis and design of mechanical systems. Part II," *ASME J. Eng. Ind.*, vol. 99, no. 3, pp. 780–784, 1977.

[11] Bauchau, O. A. and Laulusa, A., "Review of contemporary approaches for constraint enforcement in multibody systems," *Journal of Computational and Nonlinear Dynamics*, vol. 3, no. 1, p. 011005, 2008.

[12] Baumgarte, J. W., "Stabilization of constraints and integrals of motion in dynamic systems," *Comput. Methods Appl. Mech. Eng.*, vol. 1, pp. 1–16, 1972.

[13] Nikravesh, P. E., Wehage, R. A., and Kwon, O. K., "Euler parameters in computational dynamics and kinematics. part I and part II," *ASME J. Mech., Transm., Autom. Des.*, vol. 107, no. 3, pp. 358–369, 1985.

[14] Park, K. C. and Chiou, J. C., "Stabilization of computational procedures for constrained dynamical systems," *J. Guid. Control Dyn.*, vol. 11, no. 4, pp. 365–370, 1988.

[15] Bayo, E., Garca de Jaln, J., and Serna, M. A., "A modified lagrangian formulation for the dynamic analysis of constrained mechanical systems," vol. 71, pp. 183–195, 1988.

[16] Yoon, S., Howe, R. M., and Greenwood, D. T., "Geometric elimination of constraint violations in numerical simulation of Lagrangian equations," *ASME J. Mech. Des.*, vol. 116, pp. 1058–1064, 1994.

[17] Canuto, C., Hussaini, Y., Quarteroni, A., and Zang, T., *Spectral Methods: Fundamentals in Single Domains*. Springer, 2006.

[18] Fornberg, B., *A Practical Guide to Pseudospectral Methods*. Cambridge University Press, 1996.

[19] Bacelli, G. and Ringwood, J.V., "Numerical optimal control of wave energy converters," *IEEE Transactions on Sustainable Energy*, in press, 2015.

[20] Fossen, T. I., *Handbook of marine craft hydrodynamics and motion control*. Wiley, 2011.

[21] *WAMIT User Manual Version 7.0*, Incorporated and Massachusetts Institute of Technology.

[22] Ó'Catháin, M., Fossen, T. I., and Leira, B. , "Control-oriented modeling of a 2-body interconnected marine structure," in *Proc. of the IFAC MCMC'06*, Lisbon, Portugal, 2006.

[23] Shabana, A. A., *Dynamics of multibody systems*. Cambridge University Press, 2005.

[24] Elnagar, G., Kazemi, M. A., and Razzaghi, M., "The pseudospectral Legendre method for discretizing optimal control problems," *IEEE Transactions on automatic control*, vol. 40, no. 10, 1995.

[25] Ross, I. M. and Karpenko, M., "A review of pseudospectral optimal control: From theory to flight," *Annual Reviews in Control*, vol. 36, no. 2, pp. 182–197, 2012.

[26] Falcão, A., "Wave energy utilization: A review of the technologies," *Renewable and Sustainable Energy Reviews*, vol. 14, no. 3, pp. 899–918, 2010.

[27] Sea Power Ltd. Available from: http://www.seapower.ie.

[28] Ó'Catháin, M., Leira, B. J., Ringwood, J. V. , and Gilloteaux, J.-C. , "A modelling methodology for multi-body systems with application to wave-energy devices," *Ocean Engineering*, vol. 35, no. 13, pp. 1381–1387.

[29] Ó'Catháin, M., "Modelling of multibody marine systems," Master's thesis, NUI Maynooth, 2007.